ELECTRICAL ENGINEERING

(NASA-CR-120492) ANALYSIS OF AN IMPULSE NOISE SUPPRESSOR FOR FM DEMODULATORS Final Report (Auburn Univ.) 39 p HC $3.75 CSCL 09C

N75-12198

Unclas
G3/33 03543

ENGINEERING EXPERIMENT STATION
AUBURN UNIVERSITY
AUBURN, ALABAMA

ANALYSIS OF AN IMPULSE NOISE SUPPRESSOR FOR FM DEMODULATORS

Prepared by

TELEMETRY SYSTEMS LABORATORY
AUBURN UNIVERSITY
AUBURN, ALABAMA

RESEARCH PERSONNEL
Sidney N. James

FINAL REPORT
June 1, 1974

CONTRACT NAS8-20765
GEORGE C. MARSHALL SPACE FLIGHT CENTER
NATIONAL AERONAUTICS AND SPACE ADMINISTRATION
HUNTSVILLE, ALABAMA

SUBMITTED BY:

S. N. James
Assistant Professor
Co-Project Leader

APPROVED BY:

J. David Irwin
Associate Professor and Head
Electrical Engineering

FOREWORD

This technical report is the final report for contract NAS8-20765. One other technical report was submitted during the last extention of the contract which was entitled: "A Comparison of Special-Purpose and General-Purpose Computers for Data Compression" by H. C. Cobb, IV and S. N. James, November, 1973.

TABLE OF CONTENTS

LIST OF FIGURES

I. Introduction

This technical report is concerned with the evaluation of an FM click noise suppressor built by the ADCOM Corporation, Cambridge, Massachusetts under contract NAS8-21209.

Chapter II presents a short theoretical justification for the existence of FM click noise near threshold conditions. Several references are listed where more detailed theoretical analysis of click noise can be found.

Chapter III is a summary of experimental tests which were performed on this click noise suppressor. These tests were performed to verify previous test results (also included in Chapter III) and to determine the range and "worse case" type of operation for the suppressor.

Chapter IV is a summary of the conclusions reached as a result of these tests and suggestions for future work in this area.

II. Theoretical Considerations in FM Click Noise

Most modern communication theory texts include a fairly complete discussion of noise effects in FM systems including threshold and click characteristics.[1,2] This chapter is a summary of the derivations and conclusions presented in reference 1 and does not include all the details for a complete presentation.

A. Basic System

The block diagram of Fig. 2-1 shows a typical FM demodulator. The demodulation takes place from some intermediate frequency, f_i, to the baseband signal $v_o(t)$. If we assume the input signal to be of the form

$$v_i(t) = A \cos[\omega_i t + Q(t)] \tag{2-1}$$

then the output will be

$$v_o(t) = \alpha \frac{dQ(t)}{dt} \tag{2-2}$$

where α is a system constant and the message is proportional to the derivative $dQ(t)/dt$. If the modulation is such that

$$Q(t) = K \int_{-\infty}^{t} m(\lambda)d\lambda \tag{2-3}$$

then the output signal power is

$$S_o = \alpha^2 K^2 \overline{m^2(t)}. \tag{2-4}$$

B. System with Additive Noise

If an unmodulated carrier and band-limited noise is added it may be expressed in quadrature component as

$$v_i(t) = A\cos\omega_i(t) + n_c(t)\cos\omega_i t - n_s(t)\sin\omega_i t \qquad 2\text{-}5$$

or

$$v_i(t) = R(t)\cos[\omega_i t + \theta(t)] \qquad 2\text{-}6$$

where

$$R(t) = \sqrt{[A + n_c(t)]^2 + [n_s(t)]^2}$$

and

$$\theta(t) = \tan^{-1} \frac{n_s(t)}{A+n_c(t)} .$$

Assuming the noise is much less than the signal the output of the demodulator may be written as

$$n_4(t) = \frac{\alpha}{A} \frac{dn_s(t)}{dt} \qquad 2\text{-}7$$

which leads to a power density spectrum over the baseband frequency of

$$G_n(f) = \frac{\alpha^2 \omega^2}{A^2} \eta \qquad 2\text{-}8$$

for $|f| \leq \frac{B}{2}$ where $\eta/2$ is the input power density which is assumed to be white Gaussian noise over the input band-width. The output noise power is then found by integrating the power density spectrum over the

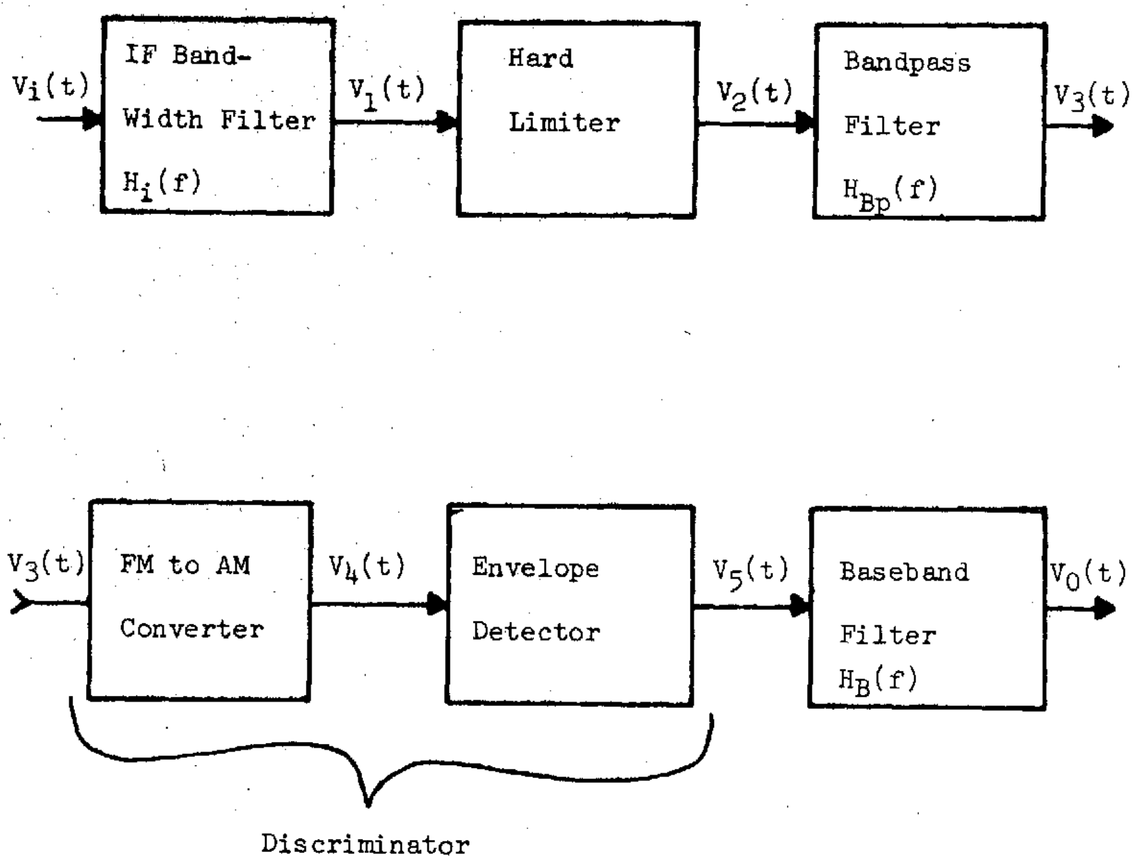

$$V_4(t) = \alpha \frac{dV_3(t)}{dt}$$

FIGURE 2-1. FM DEMODULATOR

base-band frequencies from $-f_m$ to $+f_m$:

$$N_o = \int_{-f_m}^{f_m} G_n(f)df$$

$$N_o = \frac{8\pi^2}{3} \frac{\alpha^2 \eta}{A^2} f_m{}^3. \qquad 2\text{-}9$$

An approximate signal-to-noise ratio can now be found from equation 2-4 and 2-9 as

$$\frac{S_o}{N_o} = \frac{3}{4\pi^2} \frac{K^2 \overline{m^2(t)} A^2/2}{f_m{}^2 \eta f_m} \qquad 2\text{-}10$$

If the message is assumed to be sinusoidal then

$$\frac{S_o}{N_o} = \frac{3}{2} \beta^2 \frac{S_i}{N_i} \qquad 2\text{-}11$$

where $\beta = \Delta f/fm$ is the modulation index and S_i/N_i is the input signal-to-noise ratio.

A signal-to-noise ratio gain factor may be found then as

$$\gamma = \frac{S_o/N_o}{S_i/N_i} = \frac{3}{2} \beta^2 \qquad 2\text{-}12$$

This is the type of results normally calculated to compare FM to other types of modulation and shows the improved performance expected from the wide band FM signal by trading band-width for signal-to-noise ratio gain.

This result was calculated for small additive noise and does not predict the threshold effects found when the noise level approaches the signal level.

C. Threshold Effect

As the noise level in an FM signal increases equation 2-11 predicts a linear related input and output signal-to-noise ratio. However at low signal-to-noise ratios, about 10 db, another effect takes place and that is the generation of noise impulse or clicks in addition to the expected smooth Gaussian noise.

One way of demonstrating how these impulses occur is to examine the phasor diagram of equation 2-5 or 2-6 as shown in Fig. 2-2(a) and (b). If the noise variation is small compared to the carrier amplitude A then the locus of R(t) is near A as shown in Fig. 2-2(a). This type of variation produces phase changes which are small and thus the corresponding frequency changes are small. However if the noise is large, producing a locus such as shown in Fig. 2-2(b), the phase change is 2π radians and the corresponding time derivative must change from 0 to 2π and back to 0. This results in a noise pulse in the output. More complicated phase variation which does not encircle the origin of the phasor diagram will produce impulses which are triplets or higher order impulses. Since their average value is zero and most of their harmonic content is outside the baseband filter limits they are normally not included as part of the contributing output noise.

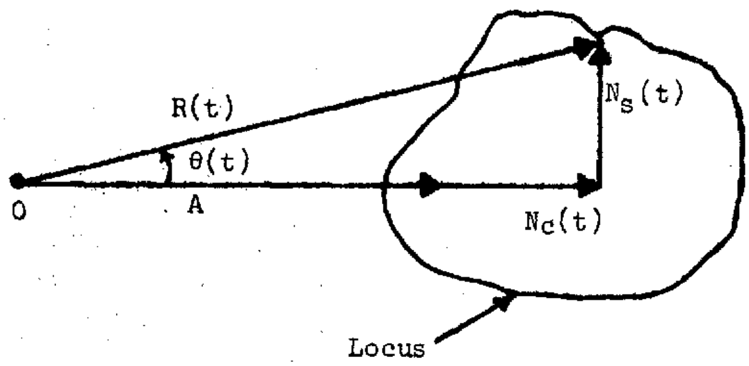

FIGURE 2-2(a). PHASOR DIAGRAM ABOVE THRESHOLD

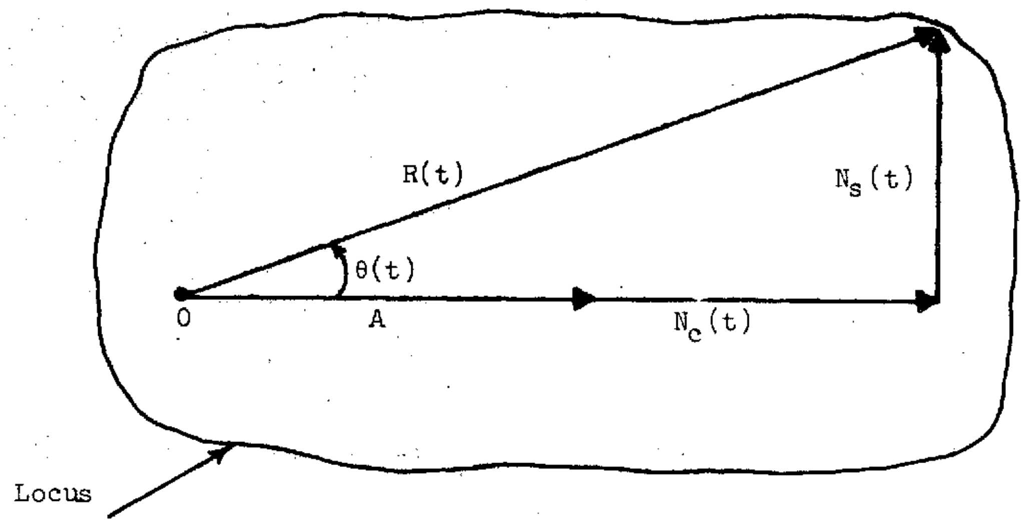

FIGURE 2-2(b). PHASOR DIAGRAM NEAR THRESHOLD

This output noise due to spikes can be calculated as

$$N_s = \frac{4\pi^2\alpha^2}{T_s} 2f_m \qquad 2\text{-}13$$

where T_s is the mean time between impulses and can be calculated as

$$\frac{1}{T_s} = \frac{B}{2\sqrt{3}} \operatorname{erf}_c \sqrt{\frac{f_m S_i}{B\ N_i}} \ . \qquad 2\text{-}14$$

Using these relations and combining both smooth Gaussian noise and impulse noise leads to a signal-to-noise ratio of

$$\frac{S_o}{N_o} = \frac{[3K^2\overline{m^2(t)}/4\pi^2 f_m](S_i/N_i)}{1+(\sqrt{3}B/f_m)(S_i/N_i)\ \operatorname{erf}_c\sqrt{(f_m/B)(S_i/N_i)}} \ . \qquad 2\text{-}15$$

This result is only valid for unmodulated carriers. If the carrier is modulated then the impulses are more frequent and the threshold effect occurs sooner as the noise increases. A typical set of output noise characteristics is shown in Fig. 2-3 where the modulation is assumed to be sinusoidal.

Several systems such as the higher order phase locked loop and the FM demodulator with feedback have been proposed to extend the threshold of FM systems.[3]

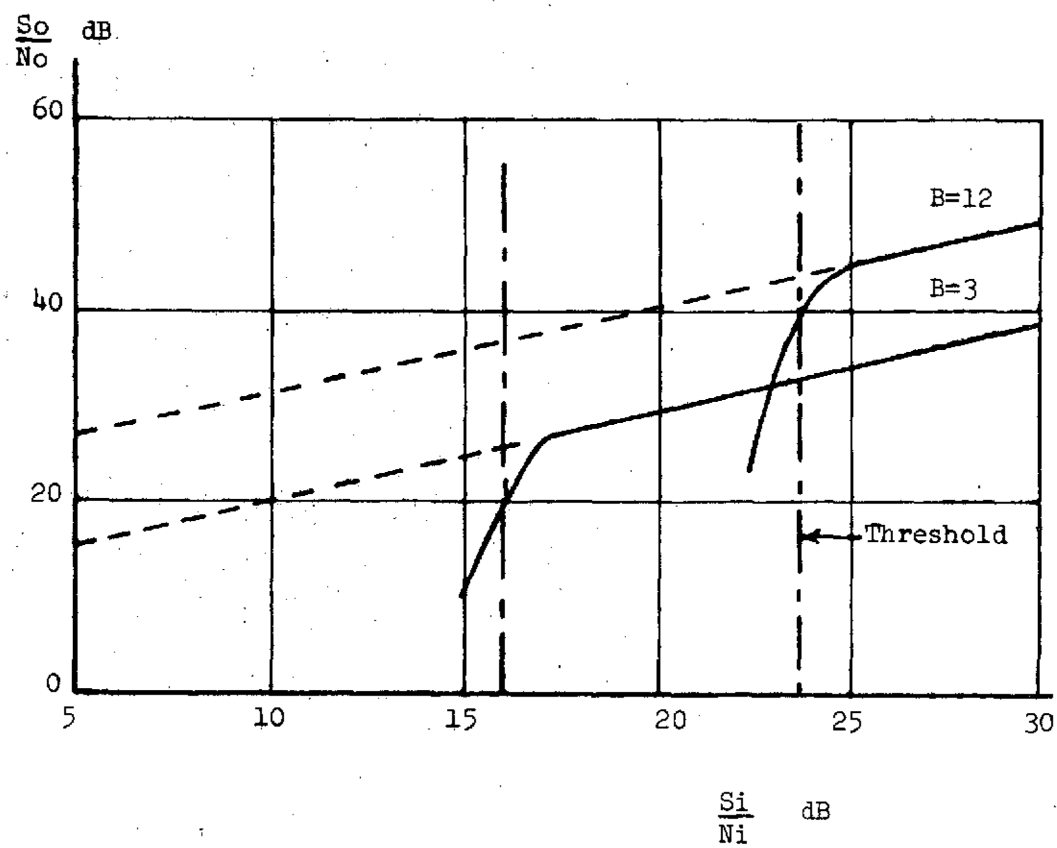

FIGURE 2-3. OUTPUT NOISE CHARACTERISTICS

III. Experimental Results Using an FM Click Suppressor

A. Previous Test Results on an FM Click Suppressor Circuit

The results presented in this section were taken from "Development and Testing of an Impulse Noise Suppressor for FM Demodulators," February 5, 1969, Contract NAS8-21209, ADCOM Corporation, Cambridge, Massachusetts. "Figure 1" shows the basic block diagram of the click suppressor and the circuit diagram is shown in "Figure 2." This circuit was used to suppress clicks generated by the test signal generator shown in "Figure 22." Note that the discriminator bandwidth was 2 MHz which is considerably larger than the IF bandwidth of 262 KHz. This was to insure that wideband clicks would be passed by the Discriminator. "Figure 3" shows typical results using the click suppressor when the carrier was modulated. "Figure 4" shows the reduction in output noise using the click suppressor for an unmodulated carrier.

B. Click Noise Generation Using the R-1037 a Telemetry Receiver

Since the same test system described in section A was not available a typical telemetry receiver (R-1037-A Telemetry Receiver by Vitro Electronics, Silver Spring, Maryland) was used. Even though this system will not generate the larger number of impulses near threshold it does present a more realistic application of the click suppressor. Figure 3-1 shows the experimental test set up used to generate the click noise. Notice that the IF bandwidth is 300 KHz but the demodulator bandwidth is 150 KHz. This demodulator bandwidth will not allow the wider bandwidth or higher order click to be passed.

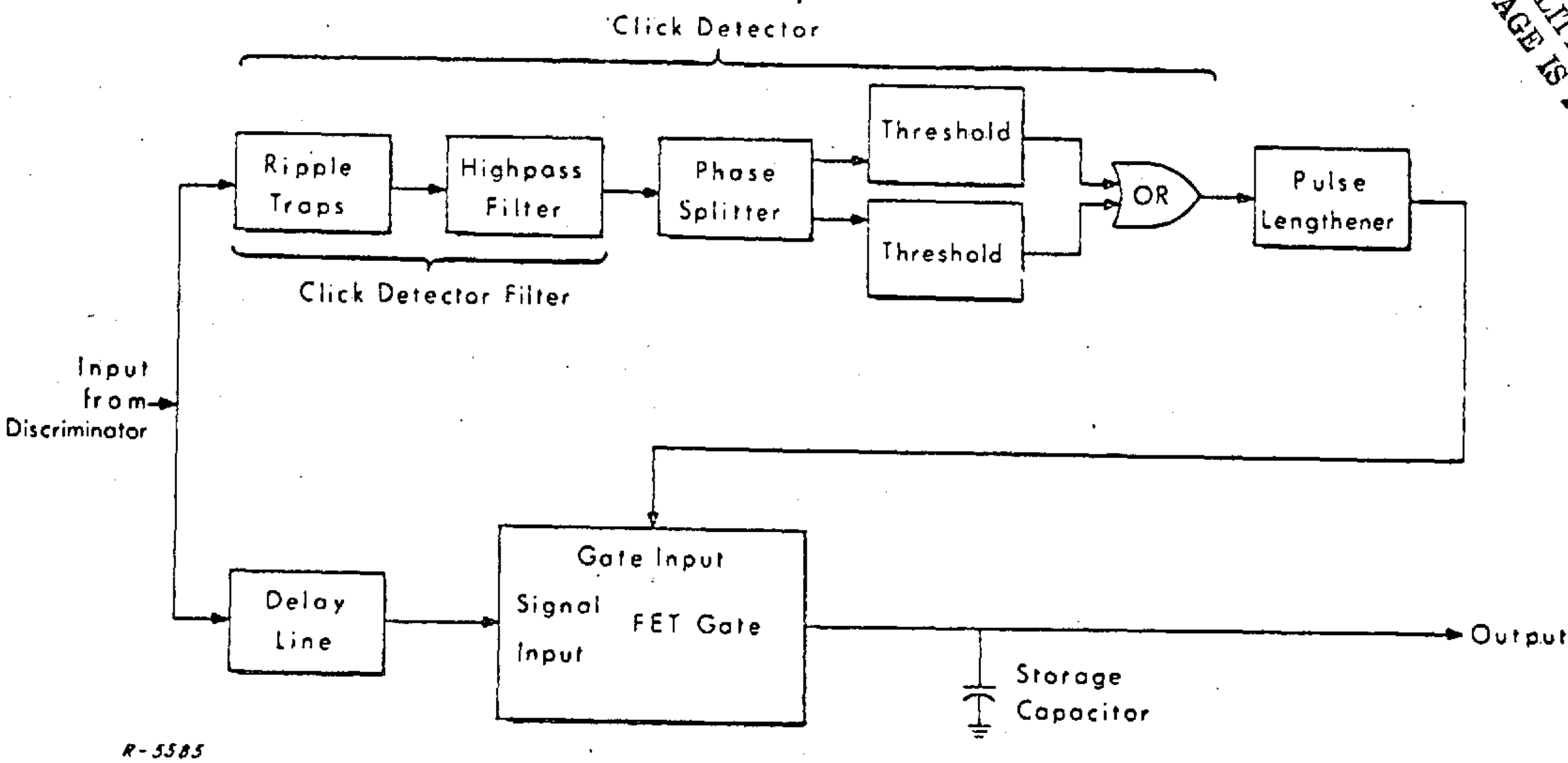

Fig. 1 Block Diagram of Click-Detecting, Signal-Holding Click Suppressor

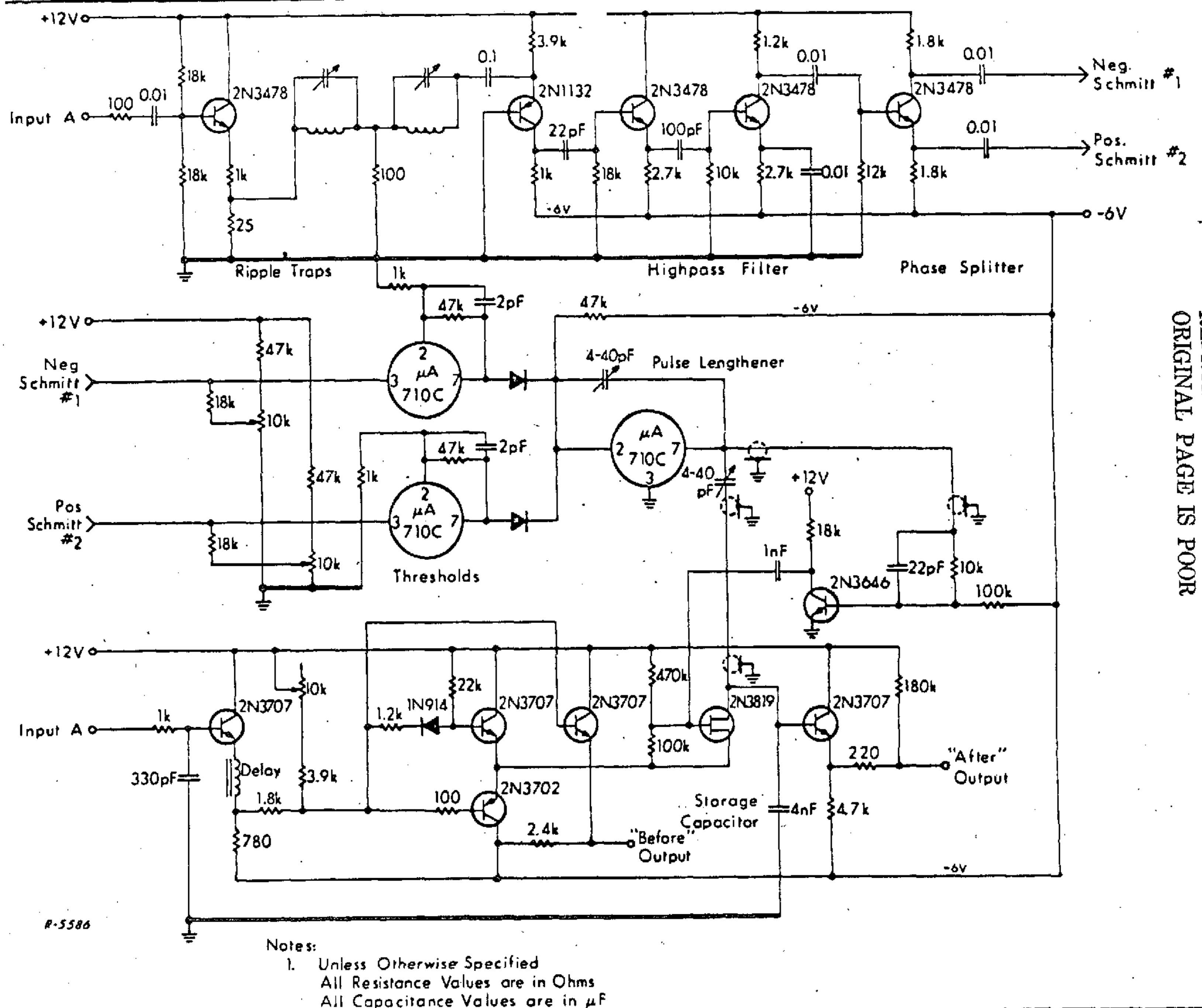

Fig. 2 Schematic of Final Click Suppressor Circuit

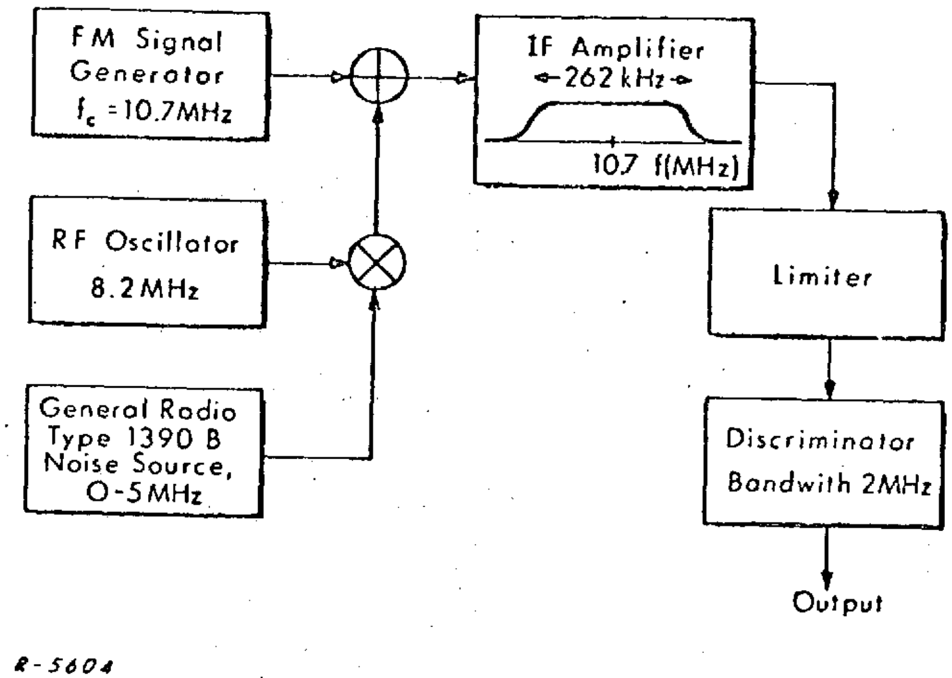

Fig. 22 Test Signal Generator

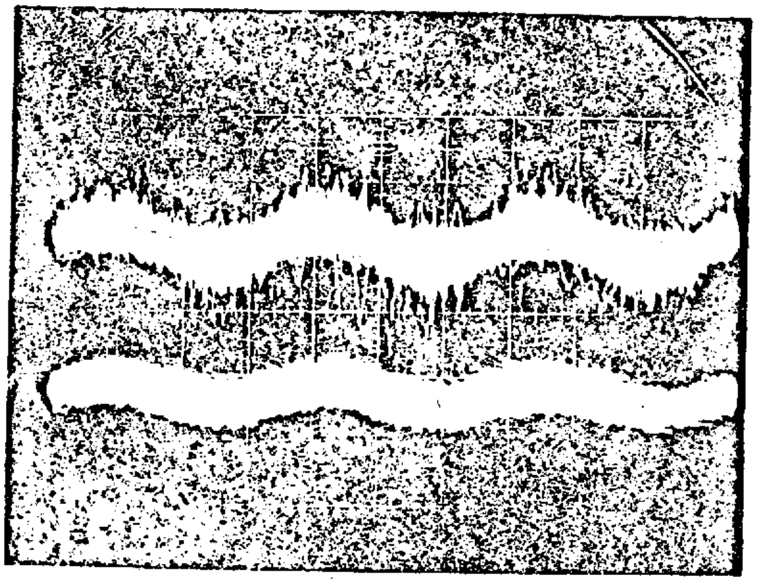

R-5587

Fig. 3 Oscilloscope Traces Before (Top) and After (Bottom) Click Suppression. The Modulation Component has the Same Amplitude in Both Traces. Modulation Frequency is 30 kHz, Derivation is ± 80 kHz, IF Bandwidth is 262 kHz, Input SNR is 5 dB.

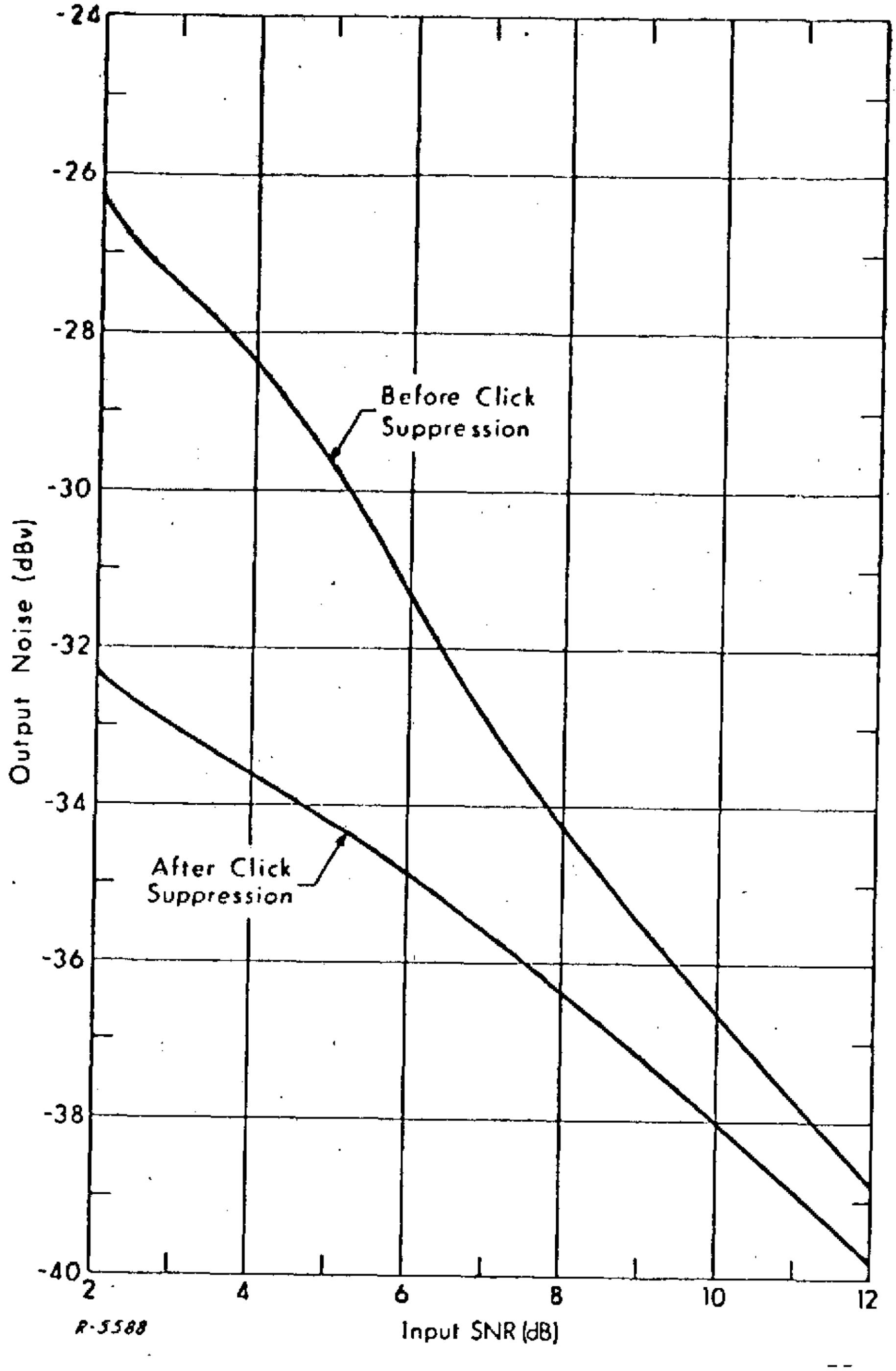

Fig. 4 Output Noise Power Before and After Click Suppression (Unmodulated Carrier)

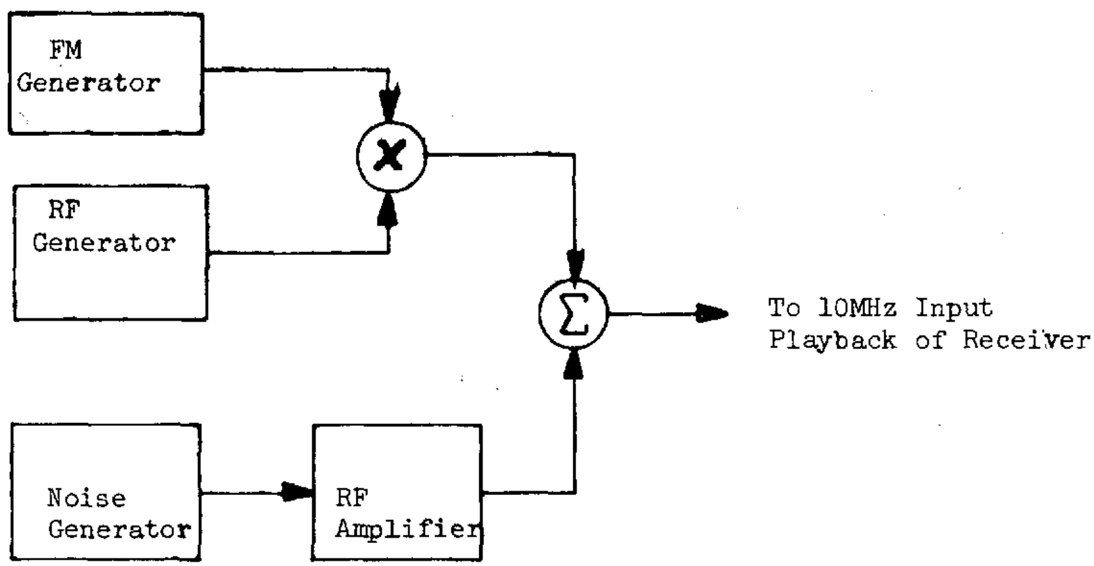

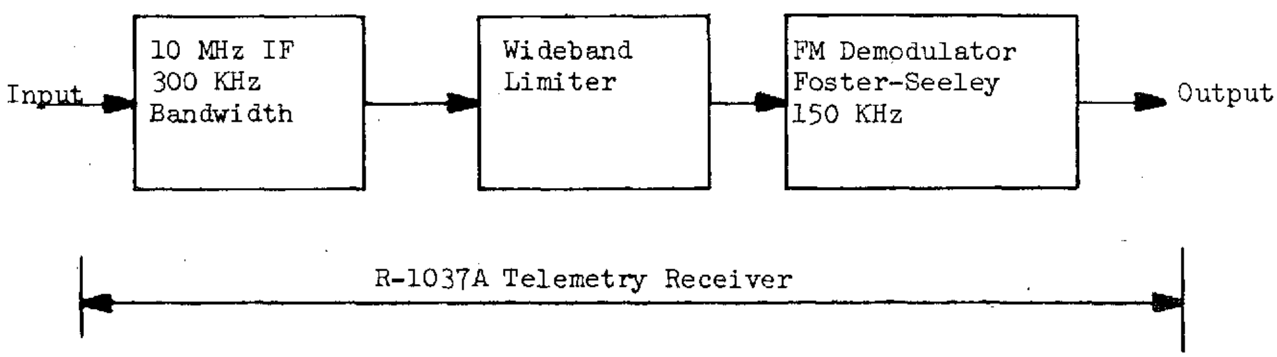

FIGURE 3-1. EXPERIMENTAL CLICK GENERATION

Figures 3-2, 3-3, 3-4 and 3-5 show typical noise characteristics near and below threshold for this receiver. Figure 3-6 shows a plot of the number of dominate clicks as a function of input signal-to-noise ratio. Since this data was taken from photographed scope traces some of the smaller clicks may have been missed.

C. Characteristics of the Click Suppressor

The click suppressor circuit shown in "Figure 2" was apparently modified before these tests were requested but the circuit operates as predicted. The major changes were the addition of two transistors, one in the high-pass filter section, and the other in the pulse shaping network and the absence of a delay element. Several different lengths of delay line were used for this element but little difference could be seen from just using a short circuit connection.

Figure 3-7 shows typical before and after click suppression results using a sine wave signal and an additive narrow pulse for click noise. The suppressor would not detect clicks longer than about 5 microseconds or smaller than about 1 volt. The signal frequency limit was about 100 KHz.

D. Click Suppression Using the R-1037-A Telemetry Receiver

Using the test system of section B and C the click suppressor was used to suppress click noise generated by a typical receiver. Figure 3-8 and 3-9 show typical before and after click suppression results. The "before" signal contains some high frequency clicks but the suppression introduces much more distortion in the signal by trying to suppress these

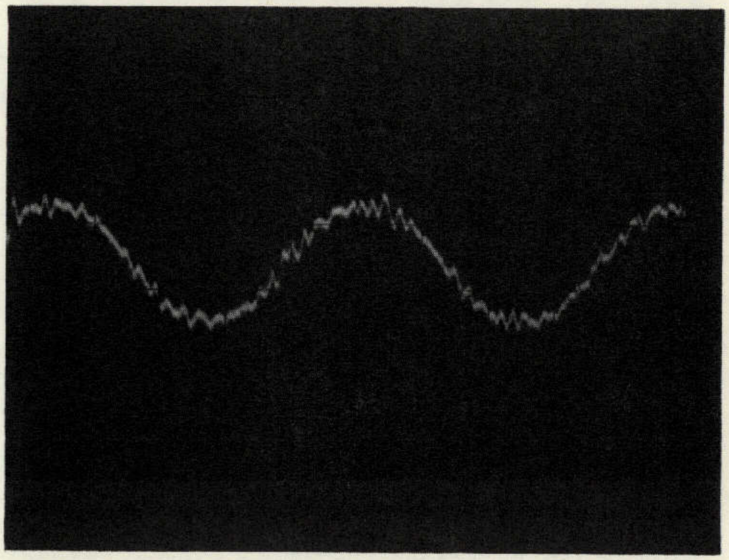

FIGURE 3-2. OUTPUT SIGNAL FOR 12 db INPUT SIGNAL-TO-NOISE RATIO, MODULATION INDEX OF 3.

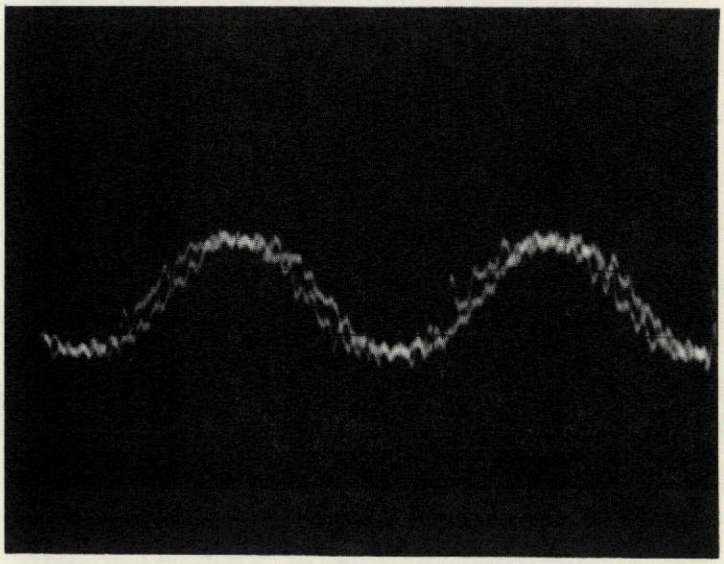

FIGURE 3-3. OUTPUT SIGNAL FOR 10 db INPUT SIGNAL-TO-NOISE RATIO, MODULATION INDEX OF 3, MULTIPLE OSCILLOSCOPE TRACES.

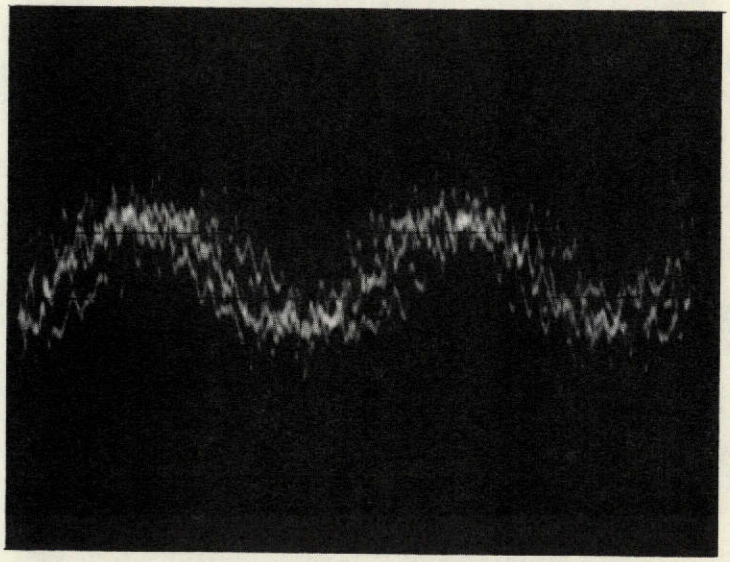

FIGURE 3-4. OUTPUT SIGNAL FOR 6 db INPUT SIGNAL-TO-NOISE RATIO, MODULATION INDEX OF 3, MULTIPLE OSCILLOSCOPE TRACES.

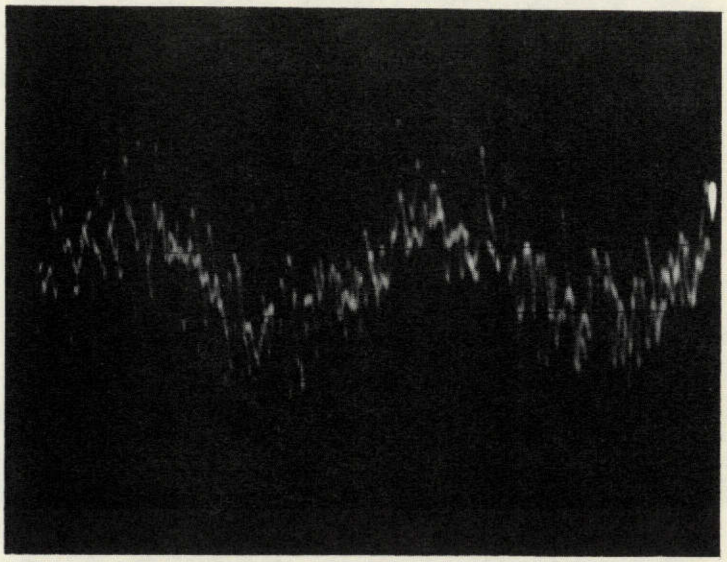

FIGURE 3-5. OUTPUT SIGNAL FOR 2 db INPUT SIGNAL-TO-NOISE RATIO, MODULATION INDEX OF 3, MULTIPLE OSCILLOSCOPE TRACES.

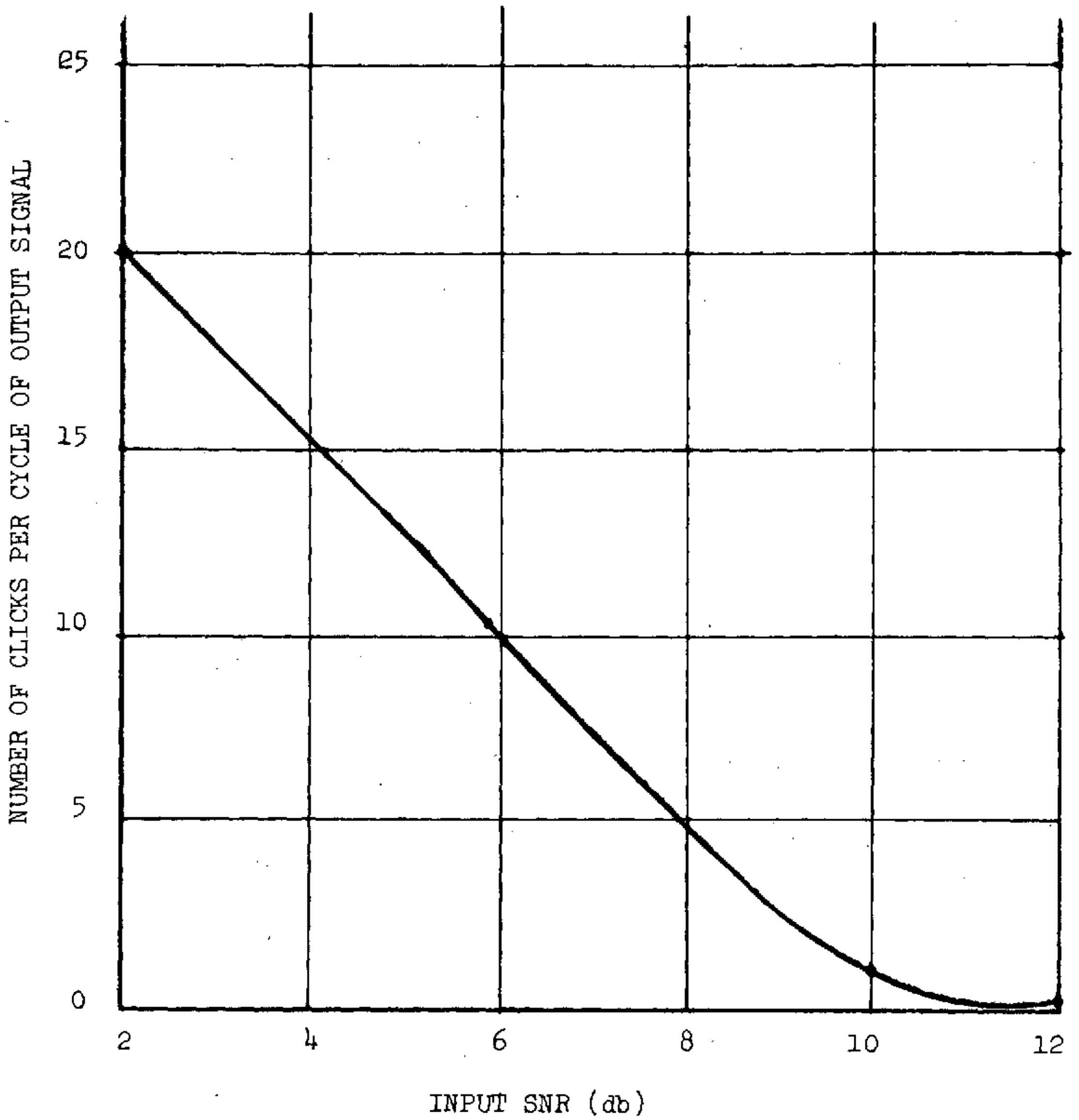

FIGURE 3-6. NUMBER OF CLICKS AS A FUNCTION
OF INPUT SIGNAL-TO-NOISE RATIO

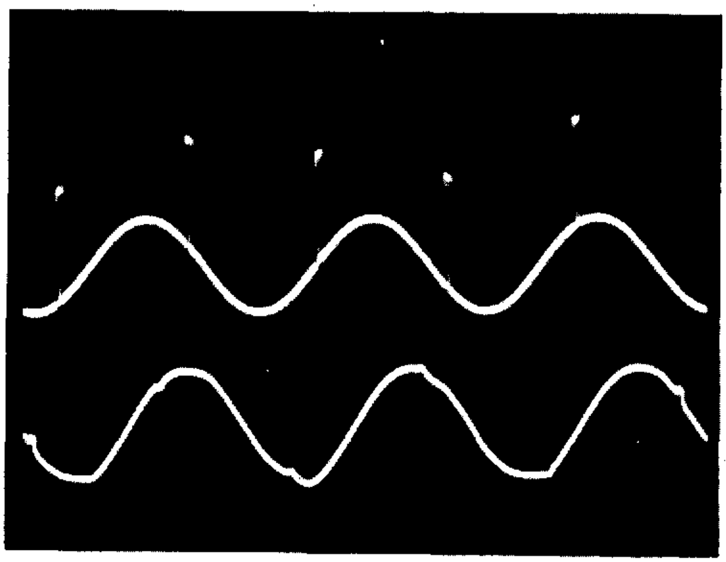

FIGURE 3-7. BEFORE AND AFTER CLICK SUPPRESSION FOR SIMULATED SIGNAL.

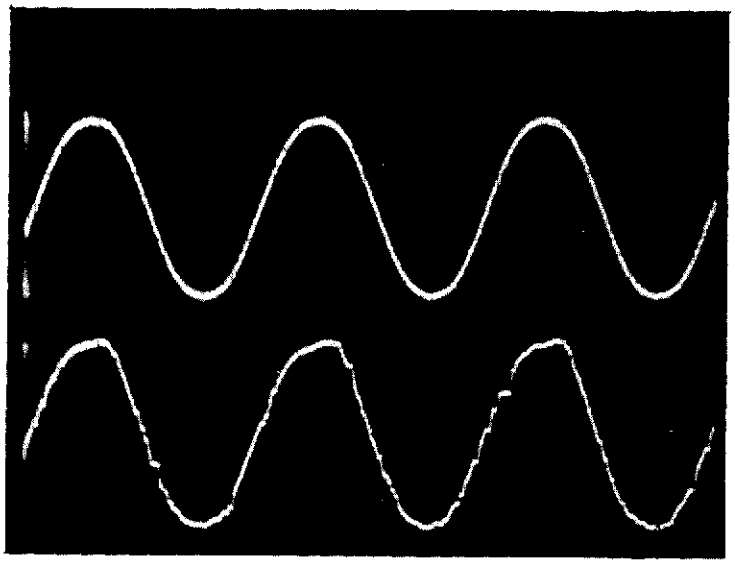

FIGURE 3-8. OUTPUT SIGNAL BEFORE (TOP TRACE) AND AFTER CLICK SUPPRESSION, 10 KHz SIGNAL AND 12 db S_i/N_i, MODULATION INDEX OF 3.

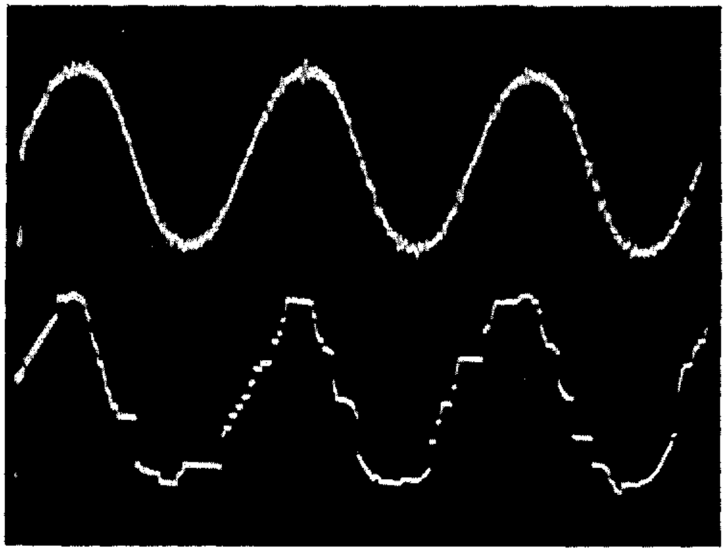

FIGURE 3-9. OUTPUT SIGNAL BEFORE (TOP TRACE) AND AFTER CLICK SUPPRESSION, 10 KHz SIGNAL AND 10 db S_i/N_i, MODULATION INDEX OF 3.

clicks. As the frequency and width of the clicks increases the signal distortion becomes very large as indicated in Figure 3-9.

Figure 3-10, 3-11 and 3-12 show output noise before and after click suppression for an unmodulated carrier. Even though the clicks are being suppressed, considerable distortion is introduced by the suppressor. Figure 3-13 is a comparison of the RMS noise voltage before and after click suppression. Here again the results show little improvement in using the click suppressor.

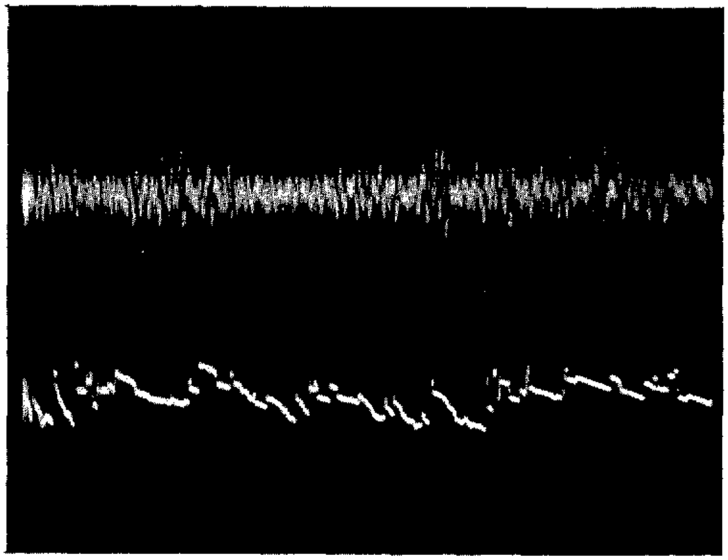

FIGURE 3-10. OUTPUT NOISE BEFORE (TOP TRACE) AND AFTER CLICK SUPPRESSION UNMODULATED CARRIER, 10 db S_i/N_i.

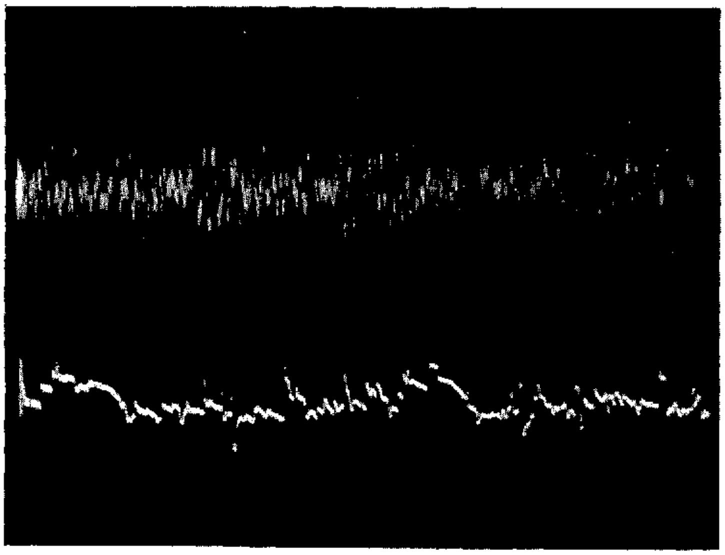

FIGURE 3-11. OUTPUT NOISE BEFORE (TOP TRACE) AND AFTER CLICK SUPPRESSION, UNMODULATED CARRIER, 6 db S_i/N_i.

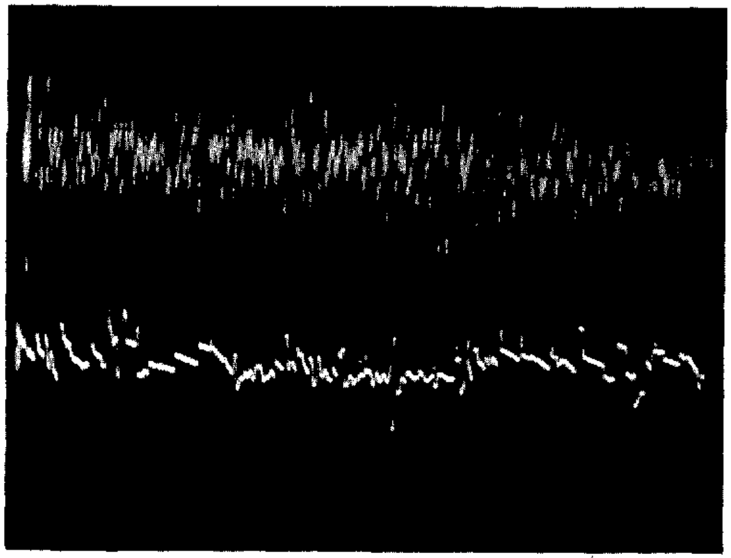

FIGURE 3-12. OUTPUT NOISE BEFORE (TOP TRACE) AND AFTER CLICK SUPPRESSION, UNMODULATED CARRIER, 2 db S_i/N_i.

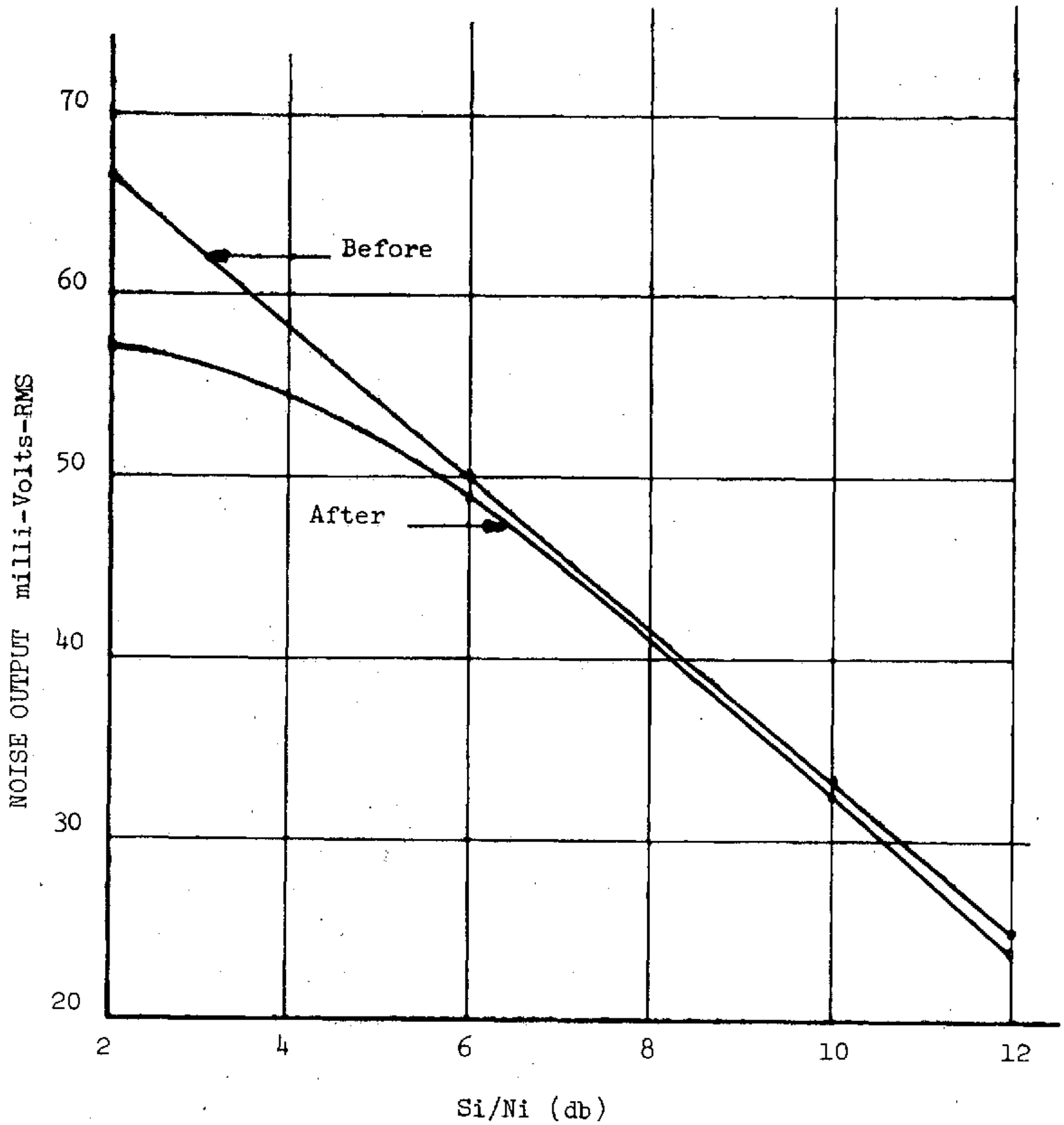

FIGURE 3-13 OUTPUT NOISE BEFORE AND AFTER CLICK SUPPRESSION FOR AN UNMODULATED CARRIER

IV. Conclusions

The initial tests on the FM click-noise suppressor show that the circuit does perform click suppression but over a limited range. Using the circuit in a practical application introduces considerable error as indicated by Figures 3-8 and 3-9. The results could probably be improved by following the suppressor with a low pass filter to smooth out the signal. Since the suppressor was designed for operation in a circuit other than the R-1037-A telemetry receiver it probably could be improved for such a specific application.

More information on the statistical characteristics of click noise is needed if an optimum suppression technique is to be designed. Information on frequency range, amplitude distribution, duration, etc. as a function of the particular system being designed would be desirable. During the performance of the experimental tests of this report many parameters were observed to affect the characteristics of the click noise.

One possible approach to better understanding the characteristics of click noise would be to study their generation using deterministic signals or simulated noise signals. This would help determine the exact time signal conditions for generating different types of clicks and how these clicks occur in different types of discriminators.

When more information on the characteristics of click noise is known, suppressor systems could be designed taking into account the discriminator as one possible choice of circuit modification as well as adding a click suppressor. Discriminators like the phase-locked-loop and demodulators with feedback should also be considered as part of an optimum suppressor design.

REFERENCES

1) Taub, H. and D. L. Schilling, Principles of Communication Systems, Chapter 10, McGraw-Hill Book Co., New York, 1971.

2) Rice, S. O., "Time-series Analysis," Chapter 25, John Wiley Inc., New York, 1963.

3) Schilling, D. D. and J. Billig, "Threshold Extension Capability of the PLL and The FMFB, Proc. IEEE, May, 1964.

4) Ringdahl, I. and D. L. Schilling, "On the Distribution of the Spikes Seen at the Output of an FM Discriminator Below Threshold," Proc. IEEE, December, 1964.